BeBeC-2014-25

ACOUSTIC WIND TUNNEL MEASUREMENTS ON A LIVE LEVEL FLIGHT PIGEON

Qingkai Wei[1], Wenjun Yu[1] and Xun Huang[1,2]
[1] Department of Aeronautics and Astronautics, College of Engineering, Peking University. 100871, Beijing, China.
[2] Airbus Noise Technology Centre, University of Southampton, Southampton, UK.

ABSTRACT

The flow-induced noise of the pigeon (*Columba livia*) during level flight is investigated with an exploratory method employed in an anechoic open-section wind tunnel. At the wind tunnel test flow of 15 m/s, a live pigeon was managed to maintain a steady level flight. A 63 channel planar microphone array parallel to the plane of pigeon wings was used to measure the sound pressure. Then, conventional beamforming method and CLEAN-SC method were adopted to yield the corresponding narrowband acoustic images and broadband sound pressure spectral results. The acoustic images show that the flight noise of the pigeon is mostly from the wing tips. In addition, the spectral waveform of the pigeon flight shows a slope of -20 dB/dec between 500 Hz and 5 kHz.

1 INTRODUCTION

The popularity of air traffic has led to serious environmental issues, in which noise is the most distinguished issue for passengers and communities local to airports. The development of high bypass ratio aero-engines has the main contributor of aircraft noise moving to the airframe for some modern transport aircrafts [11]. Since 1995, aircraft noise impact again became an issue of public interest and many researchers have focused on the reduction of airframe noise, including airfoil self-noise, landing gear and high-lift devices [3–5, 7]. Past trends in aircraft noise reduction show that those asymptotic improvements in airframe design might fail to achieve the increasingly stringent regulations and the public expectations. Hence, some aeronautic pioneers have been investigating flight noise of birds [11].

In fact, to develop various aerodynamic technologies, aviation researchers have learned from bird flight. Avian wing geometry, kinematic and aerodynamic mechanisms have been extensively studied previously, particularly for pigeons [12, 19]. In contrast, avian flight noise is still a much more open question, partially due to the absence of appropriate testing methods.

As to low noise flight of bird, owls are able to capture preys by stealthy flight. Through the morphology research of their wings, there are mainly three viewpoints of its low noise flight mechanisms: leading edge serrations, trailing edge fringes and soft upper surface of the wing. In addition, the silent flight capability of some owls is possibly attributed to low flight speed (e.g. 6∼8m/s).

In this work, we have developed experimental techniques and conducted experiments for a more readily available bird species, the pigeon (*Columba livia*), to investigate the associated flow-induced noise at a faster flight speed (15 m/s), which might yield knowledge more pertinent to future aeronautical designs.

Experiments of flyover noise [16], gliding aerodynamics [6, 15], and flapping aerodynamics [18] have been separately carried out in the free field and wind tunnels. The fly-over experiments [16] capture flight noise mechanisms with high confidence. However, it is very difficult to achieve a satisfactory signal-to-noise ratio in those field tests. On the other hand, the experimental efforts can be largely eased off using isolated dummy/specimen bird wing [9]. However, the experimental accuracy using an isolated wing of deceased birds needs justifications. In this work, the experimental method is different from those flyover noise measurements and isolated dummy/specimen wing noise measurements. We have managed to maintain the level flight of a live pigeon and then performed the flow-induced noise experiments in the anechoic, open test section wind tunnel. The experimental method and experimental results are described below.

2 EXPERIMENTAL SETUP

One white pigeon purchased from a licensed animal dealer is used to evaluate the experimental method and technique developed in this work. An external low-noise fan provides the required testing flow (the speed accuracy is within ± 0.1 m/s) through a duct to the open-jet nozzle of $0.55\text{m} \times 0.4\text{m}$ (length$\times$width). Acoustical liners have been carefully installed on the duct wall to minimize background noise while maintain flow quality. The pigeon's body is tightly and comfortably kept in a metal cage (see Fig. 1). The cage encloses the trunk with two iron rings. The diameter of the iron wire used for the iron rings is about 2 mm. Two rigid strings of 1 mm diameter connect the cage (and then the bird) to the side walls of the open test section. The entire cage can be manually adjusted to the desired flight position and attitude. Most parts of the cage are covered by contour feathers all over the trunk body and are therefore almost invisible in Fig. 1.

An array of 63 electret microphones (Panasonic WM-60A) is deployed on the ground to visualize the location and strength of flight noise sources (see Fig. 1). The microphones form multi-arm spiral lines that could largely reject spatial aliasing [10] (see Fig. 2). The sensitivity of each microphone is -45 ± 5 dBV/Pa. The frequency response (amplitude and phase) of each microphone is carefully calibrated to a Brüel & Kjær 4189 microphone with the purpose of reducing inconsistencies between array microphones. In addition, we designed high precision electronic circuits of preamplifiers to match microphone impedance and to further improve signal-to-noise ratio of the array.

The entire array was made from printed circuit board technology, which allows easy deployment and accurate mechanical specification (in the order of 0.1 mm). The diagram of the experimental setup and the coordinates used in this work are shown in Fig. 1. The experiments were carried out in an anechoic chamber room of $3.5\text{m} \times 4.5\text{m} \times 5\text{m}$ (length$\times$width$\times$height) to

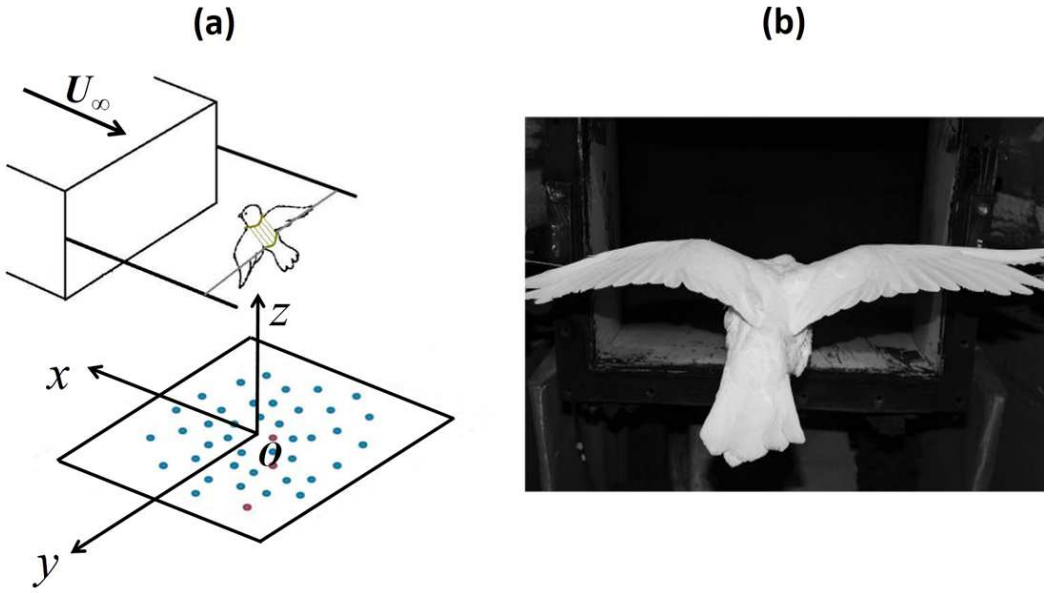

Figure 1: Experiment setup: (a) the diagram of the experimental setup; (b) image of the pigeon during the level flight at $U_\infty = 15$ m/s.

suppress acoustic reflections. The open-jet nozzle and anechoic absorbing wedges can be seen in Fig. 1 and the array can be seen in Fig. 2.

In the experiments, we fortunately found that the pigeon enjoys the level flight tests and maintains a relatively steady flight condition, which saves extensive training efforts. The test flow speed is $U_\infty = 15$ m/s. At this speed, the pigeon naturally deploys its wings and retracts its feet, as described in the literature [15]. The pigeon is not so cooperative (with struggling movements) at a higher test speed. On the other hand, the pigeon flaps wings and moves feet rapidly at a lower test speed, which calls for a real-time acoustic imaging technique, which is under developing in our laboratory. Hence, for now, the experiments are mostly conducted at 15 m/s. The experimental procedure was carried out as follows: first, the array measures noise generated during flight tests; second, flight noise distributions are determined by a classical beamforming method; and third, sound spectrum at the noise source position of interest is identified by integrating beamforming outcomes at the specific region.

The fundamentals of the classical beamforming are briefly introduced below for the completeness of this paper. Given a microphone array with M microphones, the output $\mathbf{y}(t)$ denotes time domain measurements of microphones, $\mathbf{y} \in \mathscr{R}^{M\times 1}$ and t denotes time. For a single sound source signal of interest, $x(t) \in \mathscr{R}^1$, in a free field, Green's function of the wave equation yields

$$\mathbf{y}(t) = \frac{1}{4\pi\mathbf{r}} x(t-\tau), \tau = \frac{\mathbf{r}}{C}, \tag{1}$$

where C is the speed of sound, $\mathbf{r} \in \mathscr{R}^{M\times 1}$ is the distance between the signal of interest $x(t)$ and microphones, and τ is the related propagation delay between $x(t)$ and the microphones.

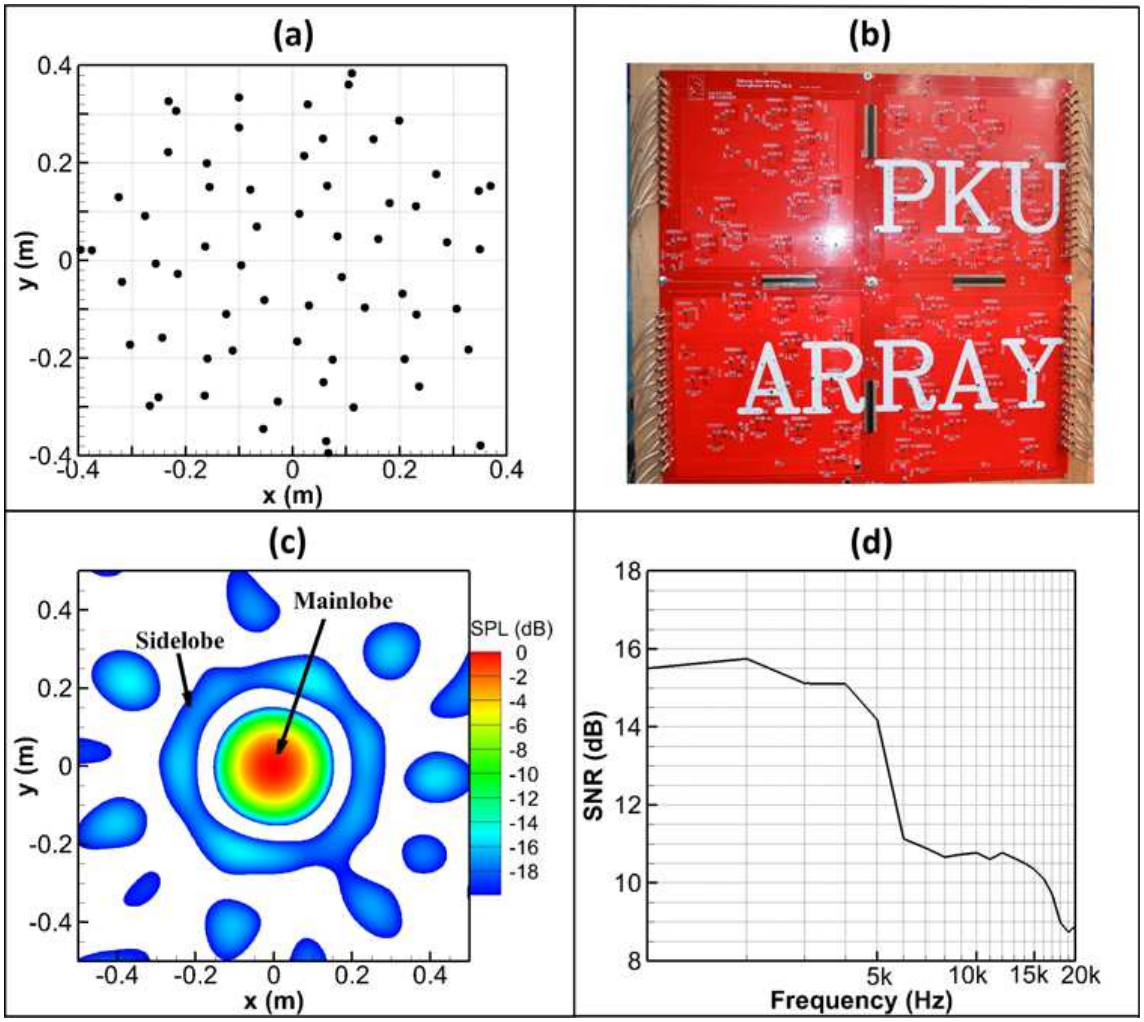

Figure 2: Array performance: (a) the layout of sensors; (b) photo of PKU Array; (c) the associated array pattern at 3 kHz; (d) the signal-to-noise ratio of the array.

Beamforming is generally conducted in the frequency domain [8], where

$$\mathbf{Y}(j\omega) = \frac{1}{4\pi\mathbf{r}} X(j\omega) e^{-j\omega\tau} = \mathbf{a}_0(\mathbf{r}, j\omega) X(j\omega), \tag{2}$$

$j = \sqrt{-1}$, $\mathbf{a}_0$ is the steering vector, and ω is angular frequency. For brevity, $(j\omega)$ and $(\mathbf{r}, j\omega)$ are omitted in the following formulations.

A narrowband beamformer output for each frequency of interest at each scanning point can be written as

$$\hat{X} = \mathbf{W}^* \hat{\mathbf{R}} \mathbf{W}, \tag{3}$$

where $\hat{X}$ is the beamformer output that estimates the sound source of interest (X); $\mathbf{W} \in \mathscr{C}^{M\times 1}$ is the beamformer weight vector; $\hat{\mathbf{R}} \in \mathscr{C}^{M\times M}$ is the cross spectral matrix, which for a total number

of I blocks, is calculated for I blocks by

$$\hat{\mathbf{R}} = \frac{1}{I}\sum_{i=1}^{I} \mathbf{Y}_i \mathbf{Y}_i^*,\ i = 1,2,3,...,I. \tag{4}$$

In these experiments, each block of data contains 4096 samples and diagonal elements of the cross spectral matrix $\hat{\mathbf{R}}$ are set as zeros to eliminate the potential influence of microphones' self noise. Then, the beamformer takes the following form,

$$\hat{X} = \frac{M^2}{M^2 - M}\mathbf{W}^*\hat{\mathbf{R}}_{\text{diag}=0}\mathbf{W}, \tag{5}$$

In addition, for the conventional beamformer of delay-and-sum type, the beamformer weight vector is obtained by

$$\min_{\mathbf{W}} \mathbf{W}^*\mathbf{W} \text{ subject to } \mathbf{W}^*\mathbf{a}_0 = 1. \tag{6}$$

The solution is $\mathbf{W_{opt}} = (\mathbf{a_0^* a_0})^{-\mathbf{1}}\mathbf{a_0}$. More details can be found in the literature [2]. The spectrum at the specified noise position can then be obtained by repeating the narrowband beamformer at frequency ranges of interest.

The distance from the test plane to the planar microphone array is almost 0.96 m. The associated array patterns at various frequencies can then be yielded. As an example, the array pattern at 3 kHz is shown in Fig. 2. The minimal amplitude difference between the mainlobe and sidelobes is used to represent the signal-to-noise ratio of the array [13]. Then, a broadband signal-to-noise ratio is examined in Fig. 2. It can be seen that the classical beamforming based on the present array design improves the signal-to-noise ratio of the flow-induced noise experiments by more than 10 dB at broad frequency ranges up to 16 kHz.

Sound refraction by the wind tunnel shear layer was corrected using the Amiet's method [1]. In this experiment, the acoustic data were prepared with a block size of 4096 at the sampling frequency of 48 kHz. Then the sample time for a single block is 0.085 s. In each experimental condition, 100 blocks were collected for each microphone channel. The resulting acoustic imaging for each narrow frequency is produced in 1/3-octave bands.

In this paper, both the conventional delay-and-sum beamforming method as described above and deconvolution method CLEAN-SC [17] were adopted to yield acoustic images in the following part.

3 RESULTS AND DISCUSSION

Some acoustic images of the pigeon's level flight noise at $U_\infty = 15$ m/s are shown in Fig. 3, from 2 kHz to 7 kHz, respectively. The direction of freestream in the figure is from right to left. Each image is achieved by processing samples of 20 blocks. We found that the bird maintains a relatively steady level flight in the associated duration. It is worthwhile to mention that the eigenvalues of cross spectral matrices for $I = 1$ to $I = 100$ have been examined, respectively, in this work to ensure the statistical confidence and incoherent background noise rejection. The anechoic facility enjoys low background noise at the test speed of $U_\infty = 15$ m/s. Hence, we found that the block number of $I = 20$ should yield imaging results with acceptable background

noise rejection. The two-dimensional imaging plane is deliberately set to the wing. It can be seen that the dynamic range of the images is 10 dB, suggesting the good quality of the experiments. The wingspan of pigeon is almost 0.5 m. In addition, Figure 4 shows the results by the advanced algorithm CLEAN-SC. The imaging results show that the dominant noise sources are at wing tips. This finding agrees with the preceding work by Geyer et al. [9]. We found the sound strength is slightly asymmetrical because it is difficult to maintain a perfectly horizontal live flight of the pigeon.

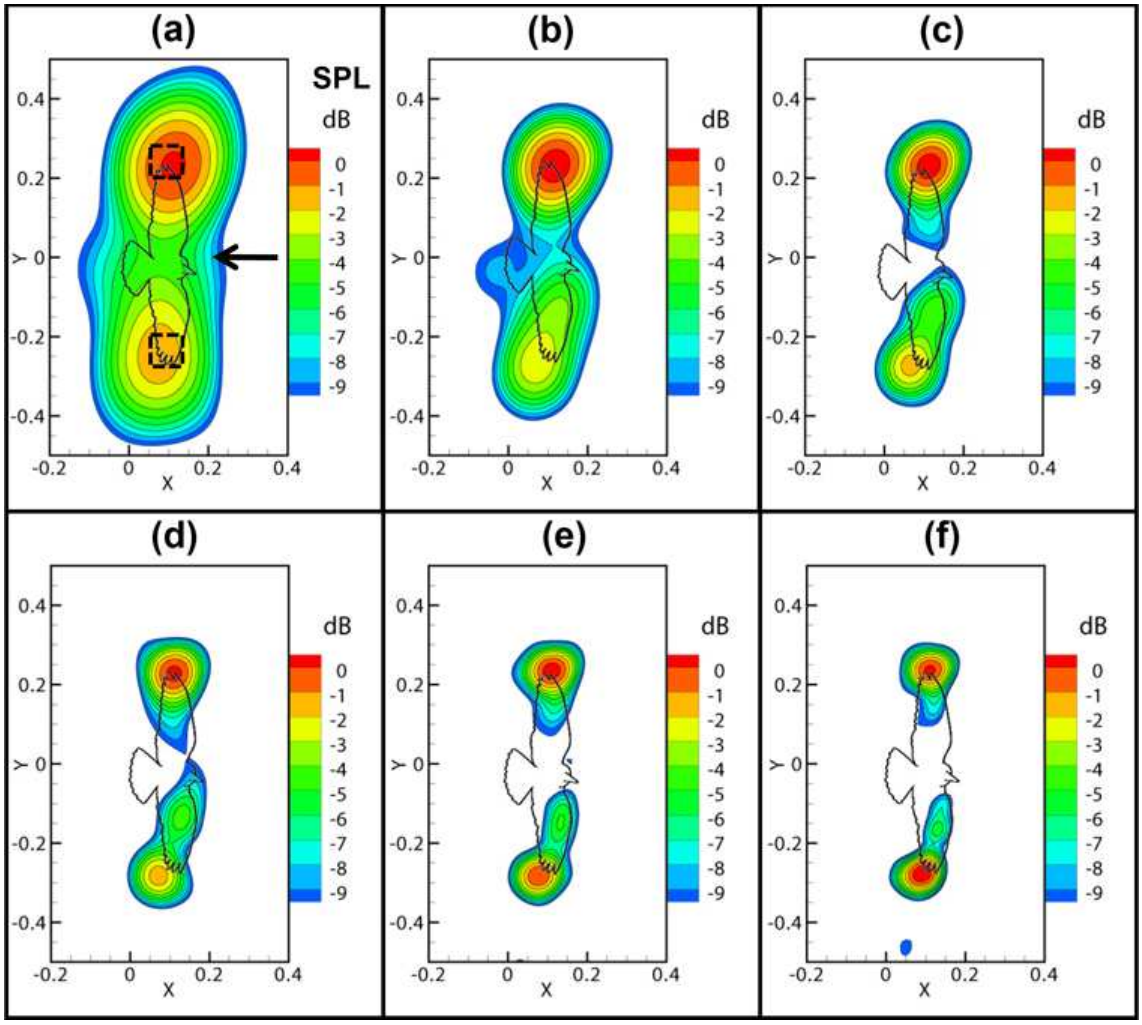

Figure 3: Acoustic image of the level flight at $U_\infty = 15$ m/s, where the imaging frequency is (a) 2 kHz, (b) 3 kHz, (c) 4 KHz, (d) 5 kHz, (e) 6 kHz and (f) 7 kHz. The maximal sound pressure value of each panel is normalized to 0 dB.

A quantitative comparison can be found in Fig. 5. Basically, the sound pressure level (SPL) of the noise source at wing tips is attained from the CLEAN-SC results. The spectra results are shown with respect to the Strouhal number, $\mathrm{St} = fL/U_\infty$, where L is the chord (0.076 m for the pigeon) and U_∞ is 15 m/s. The Mach number effect is adjusted by adopting the general

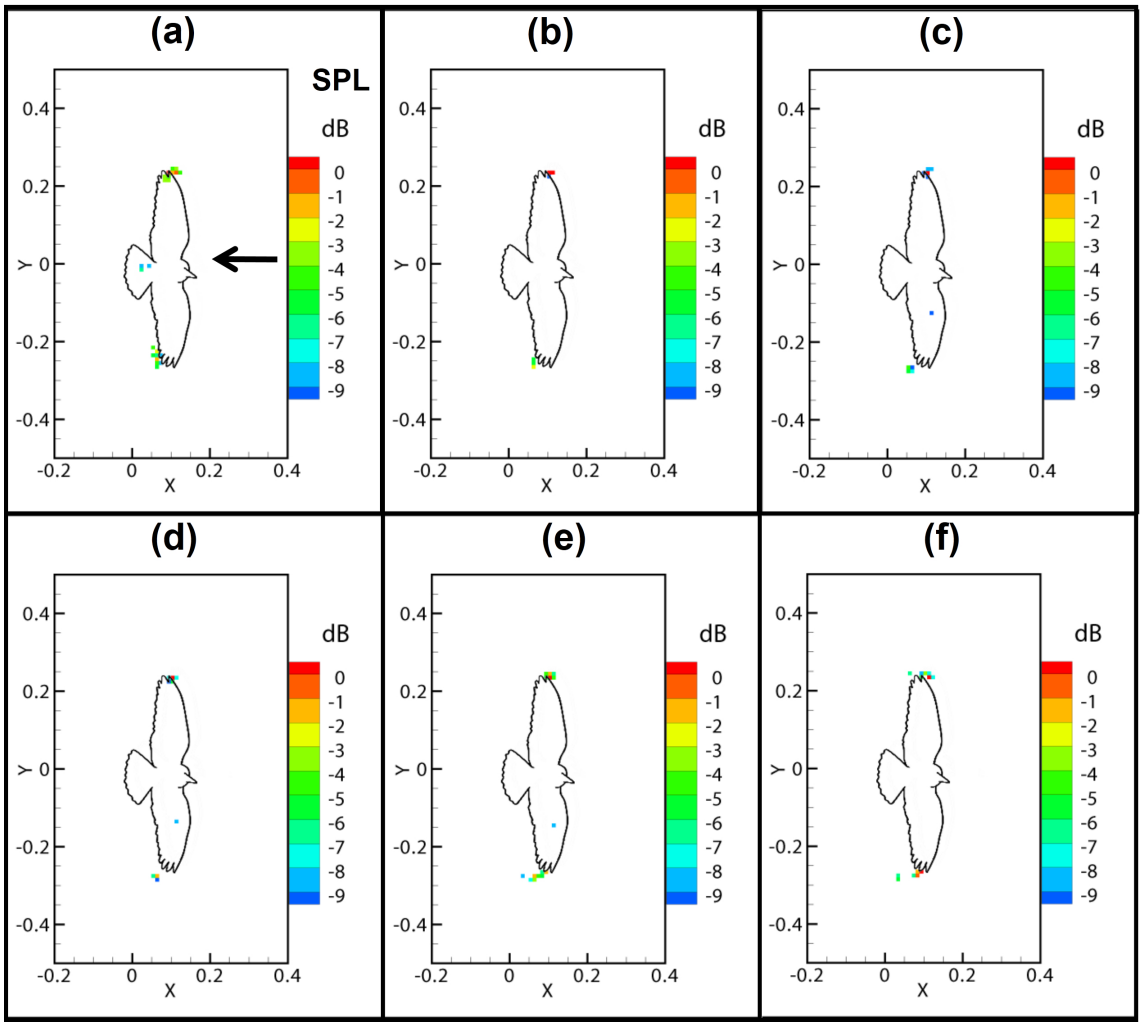

Figure 4: Acoustic image of the level flight at $U_\infty = 15$ m/s with CLEAN-SC method, where the imaging frequency is (a) 2 kHz, (b) 3 kHz, (c) 4 KHz, (d) 5 kHz, (e) 6 kHz and (f) 7 kHz. The maximal sound pressure value of each panel is normalized to 0 dB.

normalization equation for edge noise [9, 14, 16, 20],

$$\mathrm{SPL}_{\mathrm{norm}} = \mathrm{SPL} - 10\log_{10}(\mathrm{Ma})^5, \tag{7}$$

where Ma is the Mach number.

Figure 5 shows the comparison results. We should mention that the minimal test values in Geyer et al.'s pigeon test results [9] are compared with our experimental results in this figure. It can be seen that the normalized SPL waveforms are almost the same at low and middle frequency ranges. The spectral waveform of the pigeon flight suggests a slope of -20dB/dec between 500 Hz and 5 kHz, which could be different from those classical airfoil results. The understanding of the inherent physical mechanisms calls for further investigation. In addition,

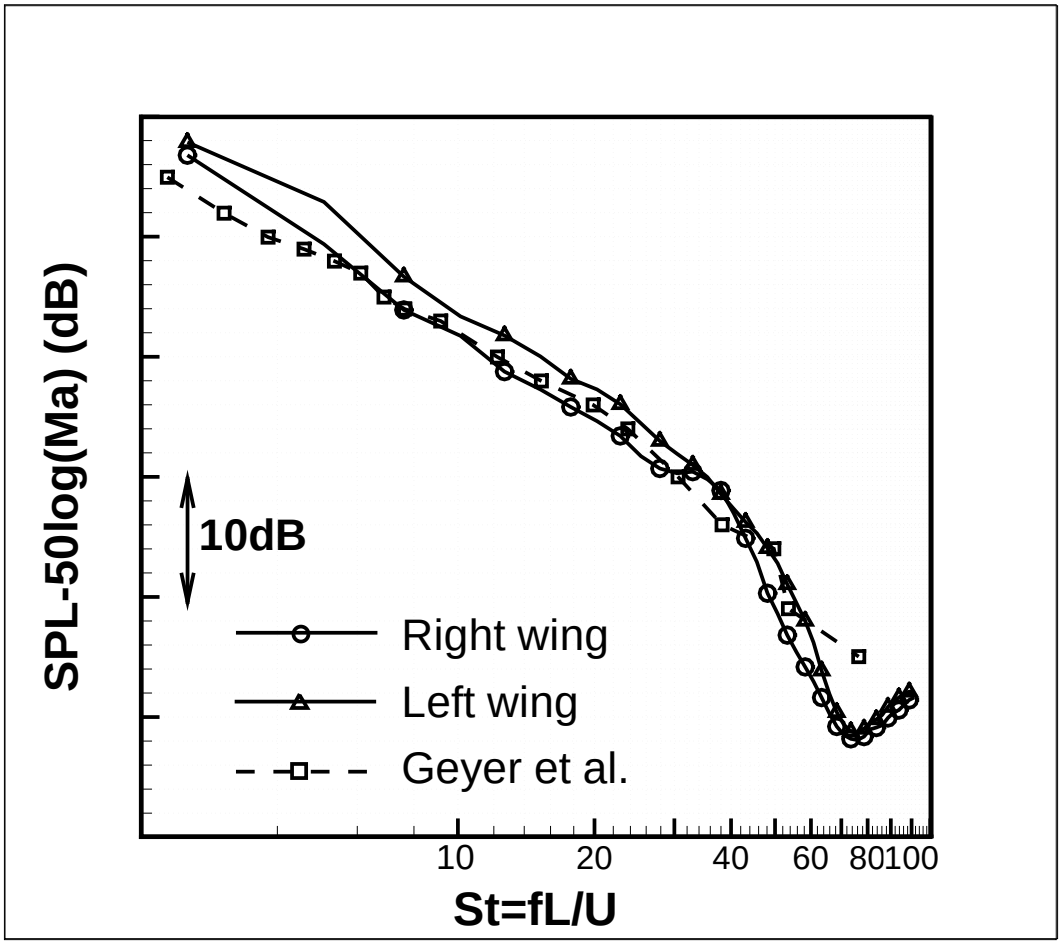

Figure 5: The live pigeon test results and the preceding results [9].

the normalized SPL results in our experiment are lower than Geyer et al.'s [9] by a couple of dB at very high frequencies beyond 10 kHz. This difference may suggest the fact that the live pigeon's wing is more effective in suppressing turbulent flow at small scales and then reducing high frequency flow-induced noise. Generally speaking, the present results agree well with the preceding experiments performed on the deceased bird model.

In summary, this work manages to perform an interesting acoustic experiment on the live pigeon. The level flight noise was studied using microphone array, classical beamforming and CLEAN-SC method. The sound spectral results agree well with preceding outcomes in the literature, justifying the proposed experimental method. Acoustic images show that the noise sources are dominant at wing tips. In contrast, for a classical airfoil, it is well known that the flow-induced noise is generally from the entire trailing edge. The understanding of inherent physical mechanisms calls for ongoing investigations.

4 ACKNOWLEDGMENTS

This research was supported by the NSF Grant of China (Grants Nos. 11172007 and 11322222) and AVIC Commercial Aircraft Engine Co., LTD.

References

[1] R. Amiet. "Refraction of sound by a shear layer." *Journal of Sound and Vibration*, 58(4), 467–482, 1978.

[2] L. Bai and X. Huang. "Observer-based beamforming algorithm for acoustic array signal processing." *Journal of Acoustical Society of America*, 130(6), 3803–3811, 2011.

[3] T. F. Brooks and W. M. Humphreys Jr. "Flap-edge aeroacoustic measurements and predictions." *Journal of Sound and Vibration*, 261(1), 31–74, 2003.

[4] T. F. Brooks and M. A. Marcolini. "Airfoil tip vortex formation noise." *AIAA Journal*, 24(2), 246–252, 1986.

[5] T. F. Brooks, D. S. Pope, and M. A. Marcolini. *Airfoil self-noise and prediction*, volume 1218. National Aeronautics and Space Administration, Office of Management, Scientific and Technical Information Division, 1989.

[6] K. Crandell and B. Tobalske. "Aerodynamics of tip-reversal upstroke in a revolving pigeon wing." *The Journal of Experimental Biology*, 214(11), 1867–1873, 2011.

[7] W. Dobrzynski. "Almost 40 years of airframe noise research: What did we achieve?" *Journal of Aircraft*, 47(2), 353–367, 2010.

[8] D. Dudgeon. "Fundamentals of digital array processing." *Proceedings of the IEEE*, 65(6), 898–904, 1977.

[9] T. Geyer, E. Sarradj, and C. Fritzsche. "Silent owl flight: acoustic wind tunnel measurements on prepared wings." *AIAA Aeroacoustics Conference*, pages AIAA 2012–2230, 2012.

[10] X. Huang, C. Xu, and L. Bai. "Is the cochlea coiled to provide sound localization?" *Europhysics Letters*, 98(5), 58002, 2012.

[11] G. Lilley. "The prediction of airframe noise and comparison with experiment." *Journal of Sound and Vibration*, 239(4), 849–859, 2001.

[12] T. Liu, K. Kuykendoll, R. Rhew, and S. Jones. "Avian wing geometry and kinematics." *AIAA Journal*, 44, 954–963, 2006.

[13] T. J. Mueller. *Aeroacoustic measurements*. Springer Verlag, 2002.

[14] S. Oerlemans and P. Migliore. "Aeroacoustic wind tunnel tests of wind turbine airfoils." *AIAA Aeroacoustics Conference*, pages AIAA 2004–3042, 2004.

[15] C. Pennycuick. "A wind-tunnel study of gliding flight in the pigeon columba livia." *The Journal of Experimental Biology*, 49, 509–526, 1968.

[16] E. Sarradj, C. Fritzsche, and T. Geyer. "Silent owl flight: bird flyover noise measurements." *AIAA Journal*, 49(4), 769–779, 2011.

[17] P. Sijtsma. "Clean based on spatial source coherence." *International Journal of Aeroacoustics*, 6(4), 357–374, 2007.

[18] J. Usherwood, T. Hedrick, C. McGowan, and A. Biewener. "Dynamic pressure maps for wings and tails of pigeons in slow, flapping flight, and their energetic implications." *The Journal of Experimental Biology*, 208(2), 355–369, 2005.

[19] D. Warrick and P. Kenneth. "Kinematic, aerodynamic and anatomical mechanisms in the slow, maneuvering flight of pigeons." *The Journal of Experimental Biology*, 201(5), 655–672, 1998.

[20] J. Williams and L. Hall. "Aerodynamic sound generation by turbulent flow in the vicinity of a scattering half plane." *Journal of Fluid Mechanics*, 40(4), 657–670, 1989.